

Published in final edited form as:

Atherosclerosis. 2009 October ; 206(2): 362–368. doi:10.1016/j.atherosclerosis.2009.03.010.

Low Vasa Vasorum Densities Correlate with Inflammation and Subintimal Thickening – Potential Role in Location-Determination of Atherogenesis

M. Gössl, M.D.¹, D. Versari, M.D.¹, L.O. Lerman, M.D., Ph.D.², A.R. Chade, M.D.², P.E. Beighley³, R. Erbel, M.D.⁴, and E.L. Ritman, M.D., Ph.D.³

¹Department of Internal Medicine, Division of Cardiovascular Diseases, Mayo Clinic College of Medicine, Rochester, MN 55905

²Division of Nephrology and Hypertension, Mayo Clinic College of Medicine, Rochester, MN 55905

³Department of Physiology and Biomedical Engineering, Mayo Clinic College of Medicine, Rochester, MN 55905

⁴University Duisburg-Essen, West German Heart Center, Hufelandstr. 55, 45122 Essen, Germany

Abstract

Objectives—To assess the role of coronary vasa vasorum (VV) spatial distribution in determining the location of early atherosclerotic lesion development.

Methods and Results—Six, 3-month old, female, crossbred swine were fed 2% high-cholesterol (HC) diet for 3 months prior to euthanasia. Six other pigs were fed normal diet (N) for the entire 6 months. Right coronary arteries were harvested and scanned intact with micro-CT (20 μ m cubic-voxel-size). After scanning, randomly selected cross-sectional histological sections were stained for nuclear-factor kappaB (NF- κ B), hypoxia-inducible factor-1 α (HIF-1 α), macrophages, von-Willebrand-factor, dihydroethidium (DHE), tumor necrosis factor- α (TNF- α) and interleukin-6 (IL-6). The number of positive stained cells, as well as intima-to-media ratio, were compared with VV density (#/mm²) obtained from micro-CT images (which closely matched the location of the histological sections) in each of four equal quadrants of the coronary vessel wall. In normal, as well as HC pigs, the number of NF- κ B ($r=0.73$ and 0.70), HIF-1 α ($r=0.74$ and 0.77), TNF- α ($r=0.58$ and 0.72) and IL-6 ($r=0.70$ and 0.72) positive cells as well as the expression of DHE (Kendall tau coefficient -0.64 and -0.63) inversely correlated with VV density. In HC the VV density also inversely correlated with intima/media ratios ($r=0.65$).

© 2009 Published by Elsevier Ireland Ltd.

Address for correspondence: Erik L. Ritman, M.D., Ph.D., Department of Physiology and Biomedical Engineering, Alfred 2-409, Mayo Clinic, 200 First Street SW, Rochester, MN 55905, USA 507-255-1933 (phone), 507-255-1935 (fax), elran@mayo.edu.

Publisher's Disclaimer: This is a PDF file of an unedited manuscript that has been accepted for publication. As a service to our customers we are providing this early version of the manuscript. The manuscript will undergo copyediting, typesetting, and review of the resulting proof before it is published in its final citable form. Please note that during the production process errors may be discovered which could affect the content, and all legal disclaimers that apply to the journal pertain.

Conclusions—Our data suggest that low-VV-density-territories within the coronary vessel wall are susceptible to hypoxia, oxidative stress and microinflammation and may therefore be starting points of early atherogenesis.

Keywords

Atherogenesis; Hypoxia; Microinflammation; Micro-CT; Vasa Vasorum

The findings of various experimental studies suggest that there is an association between vasa vasorum and atherosclerotic plaque formation. As occlusion of vasa vasorum correlates well with neointima formation¹ but inhibition of adventitial neovascularization correlates with reduced plaque growth^{2, 3} a causative role of vasa vasorum in atherosclerosis is not yet clear.

We showed recently that the distribution of coronary vasa vasorum perfusion territories throughout the coronary artery vessel wall is heterogeneous with a patchy distribution of low vasa-vasorum-density territories⁴. Since atherogenesis also occurs in a patchy pattern⁵ we hypothesized that low densities of vasa vasorum may play a role in the localization of early atherogenesis. Pivotal mechanisms of early atherogenesis in areas with a low vasa vasorum density may be the induction of microinflammation caused by hypoxia^{6, 7} and oxidative stress^{8, 9} because of decreased supply to, and decreased drainage from, the coronary vessel wall.

Using 3D micro-CT scanning techniques, in conjunction with co-registered histology and immunohistochemistry, we are able to obtain accurate quantification of vasa vasorum densities and correlate this information spatially with histological intima/media ratios and the expression of proatherogenic factors such as hypoxia-inducible factor-1alpha (HIF-1 α), the nuclear transcription factor-kappaB (NF-kB), tumor necrosis factor-alpha (TNF- α), interleukin-6 (IL-6) and in situ production of superoxide anion in the same arteries.

Hence, the current study was designed to test the hypothesis that areas of low vasa vasorum density within the coronary vessel wall show decreased oxygenation (i.e., increased expression of HIF-1 α) and increased oxidative stress (i.e., increased superoxide production) which may initiate the cascade of microinflammation (increased expression of NF-kB, TNF- α and IL-6) and subintimal proliferation, key steps in early development of coronary atherosclerosis.

METHODS

Animal Experiments and Specimen Acquisition

All animal studies were approved by the Mayo Foundation's Institutional Animal Care and Use Committee. A control group (N) of six female domestic crossbred swine were fed normal laboratory chow for six months. Six other female pigs were fed a high cholesterol diet (15% lard, 2% Cholesterol; TD 93296, Harlan Teklad, Madison, WI) for three months (group HC) prior to the study. All harvested hearts were prepared for micro-CT scanning as described previously^{4, 10, 11}. This involved injection of radio-paque Microfil® polymer into the coronary arteries prior to dissecting out five to ten cm long, intact, right coronary artery

segments (RCA). In addition, 2-cm long segments of coronaries were flash frozen in liquid nitrogen and preserved at -80°C .

Micro-Computed Tomography 3D Reconstruction

The RCA were scanned by a bench-top micro-CT system configured to generate $20\mu\text{m}$ cubic voxels¹². To preserve the connectivity of vasa vasorum, the RCA were scanned in contiguous 2-cm increments along the entire coronary artery luminal axis without physically cutting the coronary artery into pieces. The resulting 3D images were displayed using image analysis software (Analyze® 6.0™; Biomedical Imaging Resource, Mayo Clinic, Rochester, MN). Computer-generated displays of these 3D images were generated to provide different angles of view.

In-Vitro Studies

After scanning, four contiguous histological cross-sections were obtained at three random locations along each RCA (in at least 1 cm intervals). These were stained with Lawson's Elastic Van Gieson stain, NF- κB (activated subunit p65), HIF-1 α , and CD68 (for macrophages), IL-6, TNF- α and von-Willebrand-factor (F VIII). In addition, Dihydroethidium (DHE) and von-Willebrand-factor (Factor VIII) staining was also performed on fresh frozen tissue.

Lawson's Elastic Van Gieson—After micro-CT scanning, tissue sections were prepared and stained following standard protocols for Elastic van Gieson (EvG) staining¹⁰.

NF- κB , HIF-1 α , Factor VIII (von Willebrand Factor), CD68 (PG-M1 clone), Interleukin-6 (IL-6) and Tumor necrosis factor- α (TNF- α)—After preparation¹³, sections were incubated in 1:500 NF κB (RB-9034-P, Lab Vision, Fremont, CA), 1:1000 Factor VIII (A0082, DAKO Cytomation, Carpinteria, CA), 1:250 HIF-1 α (NB 100-123, clone H1 α 67-sup, NOVUS Biologicals, Littleton, CO), and anti- α -SMA (1:500; Dako Cytomation for double immunostaining), respectively; detection was completed by use of a biotin-free polymer, Mouse MACH3 (Biocare Medicals, Walnut Creek, CA) for 10 minutes or 1:100 CD68 (M0876, DAKO Cytomation, Carpinteria, CA) for 30 minutes, respectively. Sections were rinsed with TBST wash buffer. Secondary incubation with the pEnVision+/HRP labeled polymer (K4002, DAKO Cytomation) was done for 15 minutes. The slides were rinsed with TBST wash buffer. Sections were incubated in 3,3'-diaminobenzidine (DAB+)(K3467, DAKO Cytomation) or Nova Red (SK-4800, Vector Laboratories, Burlingame, CA) 5 minutes, counterstained with modified Schmidts' Hematoxylin 5 minutes followed by a 3 minute tap water rinse to blue sections, dehydration through graded alcohols, clearing in 3 changes of xylene, and mounting with a permanent mounting media.

Additional immunohistochemistry was performed using 1:500 anti-TNF- α (Serotec, MCA2360Z, Dako Cytomation for double staining with anti-Factor VIII) and 1:200 anti-IL-6 (anti-pig Clone 77830.11, R&D systems, Dako Cytomation for double staining with anti-Factor VIII). Samples of human prostate cancer (NF- κB) and tonsils (CD68, HIF-1 α , TNF- α , IL-6) served as positive controls.

After air-drying and fixation with ice-cold acetone, fresh frozen sections were stained using the protocol as described above (anti-Factor VIII), only modified appropriately for fresh-frozen tissue.

Dihydroethidium (DHE)—In situ production of superoxide anion was measured in 30- μ m frozen sections using the oxidative fluorescent dye dihydroethidium (DHE). Cytosolic DHE exhibits blue fluorescence, but once oxidized by superoxide to ethidium bromide it intercalates within the cell's DNA, staining its nucleus a fluorescent red¹³.

Western Blot—For NF- κ B analysis fresh frozen samples (n=3 per group) of epicardial coronary artery were homogenized in lysis buffer (50 mM Tris-HCl, pH 7.5, 150 mM NaCl, 1% Triton-X, 10% glycerol, 2 μ g/ml aprotinin, 1 mM PMSF) using a tissue homogenizer¹⁴. For HIF-1 α analysis, nuclear samples were isolated from fresh frozen tissue using a nuclear extraction kit (Chemicon®, Temecula, CA, n=3 per group). The lysate protein content was analyzed by Bradford assay (Bio-Rad, CA). Equal amounts of protein were diluted in 4x reducing loading buffer and boiled. Samples were then resolved in 8% SDS-polyacrylamide gels. Immunoblotting was performed using a monoclonal antibody anti HIF-1 α (1:200; Affinity Bioreagents, Golden, CO) and a polyclonal anti-NF- κ B p65 antibody (1:100, Santa Cruz Biotechnology Inc., Santa Cruz, CA) in a non-fat milk/Tris buffer; membranes were exposed to secondary antibodies, anti-mouse (1:2500, Amersham Pharmacia Biotech, Piscataway, NJ) or anti-rabbit (1:500; BD Biosciences, San Jose, CA) conjugated to horseradish peroxidase, as appropriate. After developing with chemiluminescence (Pierce, IL)¹⁴, membranes were exposed to X-ray film (Kodak, NY). Signals were evaluated for integrated density using ImageJ (National Institutes of Health). β -Actin (1:5000, Sigma-Aldrich, St. Louis, MO) was used as the loading control.

Data Analysis

Micro-CT—In each micro-CT cross-section, vessel wall area (defined by the abluminal border of the adventitia) was determined as described in detail before¹⁰ Vasa vasorum were manually identified and counted in this vessel wall area to calculate vasa vasorum density (i.e., vasa vasorum per mm² vessel wall area)¹⁰. Branching points were excluded from analysis. By scanning through the 3D data set (1000 reconstructed, contiguous, cross-sections per 2-cm of scanned coronary artery) we were able to differentiate vasa vasorum from other vessels that may have a comparable dimension but do not stay within the vascular wall (e.g., intra myocardial branches).

Analysis of Micro-CT images and their corresponding NF- κ B, HIF-1 α , TNF- α and IL-6 histology slides—Micro-CT cross-sectional images were identified that corresponded by anatomical landmarks to the histology sections taken from the same coronary (Figure 1, panels A-C). Then, ten, 21 μ m thick, contiguous micro-CT tomographic images proximal and distal to the matching image were analyzed as follows: each tomographic and histological cross section was circumferentially subdivided into four equal quadrants⁴, and vasa vasorum density calculated by manually counting the number of vasa vasorum in each vessel wall quadrant divided by its area ($\#/mm^2$, Figure 1, panel D). This provided a 3D-map of vasa vasorum densities (Figure 1, E) in close proximity to the

histology sections for later correlation (Figure 1, panel E shows the heterogeneous distribution of vasa vasorum spatial densities along the coronary artery). In the corresponding histological cross-sections stained with Elastic van Gieson the intima/media ratio was measured as an indicator of neointimal formation¹⁵. In adjacent immunohistochemistry cross-section NF- κ B, HIF-1 α , TNF- α , IL-6 and CD68 positive cells were counted in three high power-fields per quadrant (Figure 2). Finally, histology and immunohistochemistry-derived data were correlated with the mean values of vasa vasorum density per vessel wall quadrant (i.e., four data points per cross-section).

Dihydroethidium—Coronary cross sections (1/animal) were examined using a computer-aided image-analysis program (MetaMorph, Meta Imaging Series 4.6). In each representative slide, fluorescence was semiautomatically quantified in 15–20 fields by the computer program (intensity by area), and the results from all fields were averaged^{16, 17}. In sequential fresh frozen sections, vasa vasorum positive for von-Willebrand-factor (vWF, Factor VIII), and their density was correlated with DHE fluorescence using an arbitrary DHE scale (1=weak, 2=moderate, 3=strong DHE fluorescence).

Statistical Analysis

Quantitative data are presented as mean \pm SD for all arteries. Data were analyzed using unpaired *t*-test and one-way ANOVA to establish differences among groups. Correlations among the continuous variables were analyzed using a linear regression model. The Kendall tau rank correlation coefficient was used to assess the correlation between DHE grading and VV density.

A value of $P < 0.05$ was considered significant in all analyses.

RESULTS

Hypercholesterolemic pigs had significantly higher total, LDL and HDL cholesterol levels, while triglycerides and blood pressure didn't differ between the groups (Table).

Vasa vasorum density in normal and high-cholesterol coronary arteries

Vasa vasorum density (#/mm²) did not differ significantly between the two groups (N vs HC: 2.35 \pm 0.43 vs. 2.41 \pm 0.31; p =n.s.) nor did host vessel luminal radius and vessel wall area (1.52 \pm 0.23 vs. 1.44 \pm 0.15 mm and 8.15 \pm 1.89 vs. 7.89 \pm 0.82 mm²; p =n.s.).

Correlation between Vasa Vasorum Density, NF- κ B, HIF-1 α , TNF- α , IL-6 and Intima/Media Ratios

Figure 3 illustrates the strong inverse correlation between vasa vasorum density and the number of NF- κ B and HIF-1 α positive cells in normal (NF- κ B: r =-0.73, p <0.001, HIF-1 α : r =-0.74, p <0.001) and hypercholesterolemic (NF- κ B: r =-0.70, p <0.001, HIF-1 α : r =-0.77, p <0.001) coronary arteries. Hence, areas with a low number of vasa vasorum showed high numbers of NF- κ B and HIF-1 α positive cells. At high magnification those cells were identified as mainly endothelial and smooth muscle cells, which was confirmed by double immunostaining (Figure 1, online suppl.). Compared to normal, high-cholesterol arteries

showed significantly greater numbers of NF- κ B positive cells per cross section (N vs. HC: 98 ± 20 vs. 225 ± 62 ; $p<0.001$) but not of HIF-1 α positive cells (N vs. HC: 163 ± 91 vs. 121 ± 64 ; $p=n.s.$). In hypercholesterolemic arteries there was subtle subintimal thickening (expressed by intima/media ratio) that did not reach statistical significance in comparison to control arteries (N vs. HC: 0.24 ± 0.11 vs. 0.36 ± 0.14 ; $p=n.s.$). However, the intima/media ratio was inversely correlated to vasa vasorum density in hypercholesterolemic arteries (Figure 2, online suppl., HC: $r=0.65$, $p<0.001$ vs. N: $r=0.03$, $p=0.83$). In HC but not in control RCAs intima/media ratios also correlated well with the number of NF- κ B positive cells (Figure 2, online suppl., HC: $r=0.64$, $p<0.001$ vs. N: $r=0.05$, $p=0.71$). In addition, we found inverse correlations between vasa vasorum density and TNF- α and IL-6 positive cells in both, control and HC animals (Figures 3 and 4, online suppl.).

Staining for CD68 showed few macrophages in only some sections of HC animals, indicating the very early phase of atherogenesis in our porcine model. In several instances we observed that the endothelium of the main lumen but also that of vasa vasorum as well as adjacent cells within the vessel wall appeared to be involved in early inflammation (Figure 5, online suppl.).

Superoxide Production (DHE fluorescence) within the Coronary Vessel Wall

Figure 4 (A-D) shows that in the vessel wall of HC coronary arteries, superoxide production (as indicated by increased DHE fluorescence) was significantly higher than in control animals (38.5 ± 11.5 vs. 5.6 ± 4.8 % threshold area, $p<0.001$). Figure 4 (E and F) also shows that areas with lower vasa vasorum density (endothelial cell staining by factor VIII) showed increased superoxide production. Using an arbitrary scale for DHE fluorescence intensity we found a significant inverse correlation between vasa vasorum density and DHE fluorescence in normal and HC pigs (Kendall tau rank correlation coefficient -0.64 and -0.63 , respectively).

NF- κ B and HIF-1 α protein expression (Western Blotting)

Western Blot analysis confirmed the expression of NF- κ B and HIF-1 α in coronary arteries of both groups. Coronaries of the HC group showed significantly higher expression of both proteins compared to control coronaries (Figure 6, online suppl.).

DISCUSSION

This study demonstrates that in control and high cholesterol animals coronary vessel wall regions with low vasa vasorum spatial densities show increased hypoxia, oxidative stress, microinflammation and early subintimal thickening.

Direct correlation of histology/immunohistochemistry data with the vasa vasorum density derived from corresponding micro-CT cross-sections revealed significant, inverse correlations between vasa vasorum density, NF- κ B, HIF-1 α , TNF- α and IL-6 positive cells. In addition, in hypercholesterolemic pigs, which showed subtle subintimal thickening, intima/media ratios also were inversely correlated to vasa vasorum density. This new information indicates that the inherently heterogeneous, patchy distribution of vasa vasorum spatial densities within the coronary vessel wall, which can already be observed in coronary

arteries of 1-month-old piglets¹⁸, may be a morpho-anatomical factor determining the location of atherogenesis⁴. Groszek and Grundy speculated 1980 that atherogenesis occurs in vessel wall areas with a relative paucity of vasa vasorum due to a decreased efflux of lipoproteins from the artery wall¹⁹. The current study demonstrates that vessel wall areas with a low number of vasa vasorum show impaired oxygenation, demonstrated by the increased number of HIF-1 α positive cells. In addition, these areas also showed increased levels of oxidative stress (DHE staining) and signs of microinflammation (NF- κ B, TNF- α , IL-6 staining). The activation of NF- κ B in this early phase may be stimulated by local hypoxia and accumulation of oxidized metabolites leading to increased oxidative stress. This results in the translocation of NF- κ B to the nucleus, binding of DNA and activation of the transcription of specific genes which others suggest finally leads to the expression of cytokines, adhesion molecules and enzymes, which have an important role in inflammation and proliferation²⁰⁻²². Based on these observations we hypothesize that the increased activation of NF- κ B in vessel wall areas with low vasa vasorum densities, leads to an accentuated attraction of further pro-atherogenic factors into these vessel wall areas. This hypothesis is supported by our finding that in hypercholesterolemic RCAs the number of NF- κ B positive cells correlated with early subintimal proliferation. The normal, heterogeneous distribution of vasa vasorum spatial densities that we find in all porcine coronary arteries⁴, even in 1-month-old piglets¹⁸, may, therefore, greatly influence the subsequent heterogeneous distribution of atherosclerosis. Fewer coronary artery vasa vasorum (both venous and arterial⁴) means less supply to, and drainage from, that specific region of the coronary vessel wall. Conceivably, during exposure to cardiovascular risk factors, pro-atherosclerotic substances, like oxLDL, can accumulate here due to decreased venous draining and induce microinflammation and finally neointima formation²³. The decreased oxygen/nutrient supply due to fewer arterial vasa vasorum potentiates this process further, as previously alluded to in experiments performed by Barker and coworkers¹. In those experiments the selective occlusion of arterial vasa vasorum of porcine femoral arteries was associated with intimal hyperplasia.

In the more advanced atherosclerotic process, when the atherosclerotic lesion progresses, angiogenic factors are released, and eventually lead to vasa vasorum neovascularization²⁴. In this situation, higher densities of vasa vasorum may actually aggravate the atherosclerotic process as suggested by the histology-based results of Moulton et al.^{2, 3}. In those experiments the inhibition of angiogenesis reduced plaque growth in hypercholesterolemic apoE $-/-$ mice supporting a role of vasa vasorum as entry ports for proatherosclerotic cellular and non-cellular blood components. Indeed, we also occasionally observed histological evidence of early inflammation in the close proximity of the vasa vasorum in hypercholesterolemia (Figure 5, online suppl.).

In the current study, however, we evaluated specifically atherogenesis at a very early stage, which is also indicated by the non-significant increase in intima-media ratio.

There are only limited data in the literature analyzing the immediate spatial relationship of vasa vasorum and atherosclerosis, let alone early atherogenesis. Schuette et al.²⁵ found no relationship between the distribution of vasa vasorum in the aortic wall and the predilected areas of atherosclerotic plaques in the human aorta using India ink injections. However, they

used human aortae obtained from autopsy where atherosclerotic plaques had already developed. It is likely that these data did not fully reflect the early process of plaque development as more recent work has documented that atherosclerotic plaques lead to vasa vasorum neovascularization^{3, 24}.

The current study shows that pro-atherogenic oxidative stress and microinflammation are heterogeneously distributed within the coronary vessel wall and spatially related to the heterogeneous distribution of vasa vasorum spatial densities. Moreover, we could demonstrate that these processes already start in the normal coronary artery wall and are further enhanced by atherosclerotic risk factors like hypercholesterolemia even before the development of significant intima-media remodeling. Nevertheless, early subintimal proliferation was also inversely related to vasa vasorum density and accompanying vessel wall microinflammation.

We obtained a 3D-map of vasa vasorum densities from a stack of contiguous micro-CT cross-sections surrounding the location of the corresponding histology/immunohistochemistry sections. Thus, the derived vasa vasorum densities (from non-distorted, vessel-continuity-preserving micro-CT data) reflect vasa vasorum 3D spatial anatomy. The thereby-obtained density data are more accurate and reliable than data from single, non-contiguous, sections from conventional histology, in that the absence of vasa vasorum in 3D micro-CT images is more likely to be representative of the local situation than absence of vasa vasorum in a few separated histology sections.

In contrast to micro-CT data derived from the LAD microcirculation in younger female pigs, with higher cholesterol levels²⁶, we did not see vasa vasorum neovascularization in high-cholesterol RCAs (LADs from the pigs of our current study were used for additional experiments including Western Blotting which excluded an appropriate Microfil preparation for Micro-CT scanning). Another possible explanation for this delay in vasa vasorum neovascularization is also the different hemodynamic environment the RCA is subjected to. In contrast to the left coronary bed, the RCA's ratio of systolic to diastolic flow at rest is substantially greater²⁷. Nevertheless, the absence of RCA vasa vasorum neovascularization observed in the current study (but may have developed at a later time) offered the opportunity to assess the described vessel wall processes dissociated from neo-angiogenesis and, hence, in the very early phase of atherogenesis. Based on our current and earlier micro-CT studies in control pigs (newborn piglets¹⁸ and pigs of up to 6 months of age) demonstrating an inherently patchy, non-uniform, spatial distribution of low vasa vasorum density territories in all coronary arteries it is very unlikely that these low vasa vasorum densities are the result of atherosclerosis, especially since our animal model is a model of early atherosclerosis. Further studies have to show if there is a differential reaction to angiogenic stimuli between different coronary vascular beds possibly based on additional anatomical and functional differences (shear stress, flow patterns, mechanical forces, intramyocardial compression²⁷), age²⁸ and maturation¹⁸.

The conclusions presented here are limited to our observations in 12 pigs. Studies with a larger number of pigs and/or animal models may be necessary to confirm our results.

Supplementary Material

Refer to Web version on PubMed Central for supplementary material.

Acknowledgments

The study was supported in part by the National Institutes of Health (grants HL-65342 and EB-000305). We thank Jill L. Anderson for helping with the animal studies, James D. Krier for helping with the DHE stains, Andrew J. Vercnocke for the micro-CT image reconstruction, Steven M. Jorgensen and David F. Hansen for the micro-CT scans and Diane R. Eaker for programming. The authors want to thank Dr. Mair Zamir (University of Western Ontario, London, Ontario, Canada) for his helpful comments in editing this manuscript.

Drs. D. Versari, L.O. Lerman, A.R. Chade, and R. Erbel contributed significant intellectual input to the design of the conducted experiments and the composition of this manuscript. Ms. P.E. Beighley was heavily involved in the animal experiments, tissue preparation and micro CT scanning process. Drs. M. Gössl and E.L. Ritman designed the study protocol, conducted all animal experiments, did the data analysis and wrote this manuscript.

In memoriam of Ms. Patricia Beighley who died November 23rd 2008.

REFERENCES

1. Barker SG, Talbert A, Cottam S, Baskerville PA, Martin JF. Arterial intimal hyperplasia after occlusion of the adventitial vasa vasorum in the pig. *Arterioscler Thromb*. 1993; 13:70–77. [PubMed: 8422341]
2. Moulton KS, Heller E, Konerding MA, Flynn E, Palinski W, Folkman J. Angiogenesis inhibitors endostatin or TNP-470 reduce intimal neovascularization and plaque growth in apolipoprotein E-deficient mice. *Circulation*. 1999; 99:1726–1732. [PubMed: 10190883]
3. Moulton KS, Vakili K, Zurakowski D, Soliman M, Butterfield C, Sylvain E, Lo KM, Gillies S, Javaherian K, Folkman J. Inhibition of plaque neovascularization reduces macrophage accumulation and progression of advanced atherosclerosis. *Proc Natl Acad Sci U S A*. 2003; 100:4736–4741. [PubMed: 12682294]
4. Gössl M, Malyar NM, Rosol M, Beighley PE, Ritman EL. Impact of coronary vasa vasorum functional structure on coronary vessel wall perfusion distribution. *American journal of physiology*. 2003; 285:H2019–2026. [PubMed: 12855425]
5. McGill HC Jr, McMahan CA, Zieske AW, Malcom GT, Tracy RE, Strong JP. Effects of nonlipid risk factors on atherosclerosis in youth with a favorable lipoprotein profile. *Circulation*. 2001; 103:1546–1550. [PubMed: 11257083]
6. Schmedtje JF Jr, Ji YS, Liu WL, DuBois RN, Runge MS. Hypoxia induces cyclooxygenase-2 via the NF-kappaB p65 transcription factor in human vascular endothelial cells. *J Biol Chem*. 1997; 272:601–608. [PubMed: 8995303]
7. Harris AL. Hypoxia--a key regulatory factor in tumour growth. *Nat Rev Cancer*. 2002; 2:38–47. [PubMed: 11902584]
8. Rodriguez-Porcel M, Lerman LO, Holmes DR Jr, Richardson D, Napoli C, Lerman A. Chronic antioxidant supplementation attenuates nuclear factor-kappa B activation and preserves endothelial function in hypercholesterolemic pigs. *Cardiovasc Res*. 2002; 53:1010–1018. [PubMed: 11922911]
9. Collins T, Cybulsky MI. NF-kappaB: pivotal mediator or innocent bystander in atherogenesis? *J Clin Invest*. 2001; 107:255–264. [PubMed: 11160146]
10. Gössl M, Rosol M, Malyar NM, Fitzpatrick LA, Beighley PE, Zamir M, Ritman EL. Functional anatomy and hemodynamic characteristics of vasa vasorum in the walls of porcine coronary arteries. *The anatomical record*. 2003; 272:526–537. [PubMed: 12740947]
11. Gössl M, Versari D, Mannheim D, Ritman EL, Lerman LO, Lerman A. Increased spatial vasa vasorum density in the proximal LAD in hypercholesterolemia--implications for vulnerable plaque-development. *Atherosclerosis*. 2007; 192:246–252. [PubMed: 16919638]
12. Jorgensen SM, Demirkaya O, Ritman EL. Three-dimensional imaging of vasculature and parenchyma in intact rodent organs with X-ray micro-CT. *Am J Physiol*. 1998; 275:H1103–1114. [PubMed: 9724319]

13. Chade AR, Krier JD, Rodriguez-Porcel M, Breen JF, McKusick MA, Lerman A, Lerman LO. Comparison of acute and chronic antioxidant interventions in experimental renovascular disease. *Am J Physiol Renal Physiol.* 2004; 286:F1079–1086. [PubMed: 14722019]
14. Wilson SH, Caplice NM, Simari RD, Holmes DR Jr, Carlson PJ, Lerman A. Activated nuclear factor-kappaB is present in the coronary vasculature in experimental hypercholesterolemia. *Atherosclerosis.* 2000; 148:23–30. [PubMed: 10580167]
15. van Royen N, Hoefer I, Bottinger M, Hua J, Grundmann S, Voskuil M, Bode C, Schaper W, Buschmann I, Piek JJ. Local monocyte chemoattractant protein-1 therapy increases collateral artery formation in apolipoprotein E-deficient mice but induces systemic monocytic CD11b expression, neointimal formation, and plaque progression. *Circ Res.* 2003; 92:218–225. [PubMed: 12574150]
16. Chade AR, Rodriguez-Porcel M, Grande JP, Krier JD, Lerman A, Romero JC, Napoli C, Lerman LO. Distinct renal injury in early atherosclerosis and renovascular disease. *Circulation.* 2002; 106:1165–1171. [PubMed: 12196346]
17. Chade AR, Rodriguez-Porcel M, Grande JP, Zhu X, Sica V, Napoli C, Sawamura T, Textor SC, Lerman A, Lerman LO. Mechanisms of renal structural alterations in combined hypercholesterolemia and renal artery stenosis. *Arteriosclerosis, thrombosis, and vascular biology.* 2003; 23:1295–1301.
18. Goss M, Zamir M, Ritman EL. Vasa vasorum growth in the coronary arteries of newborn pigs. *Anat Embryol.* 2004; 208(5):351–357. [PubMed: 15309629]
19. Groszek E, Grundy SM. The possible role of the arterial microcirculation in the pathogenesis of atherosclerosis. *J Chronic Dis.* 1980; 33:679–684. [PubMed: 7430319]
20. Baeuerle PA, Henkel T. Function and activation of NF-kappa B in the immune system. *Annu Rev Immunol.* 1994; 12:141–179. [PubMed: 8011280]
21. Levkau B, Scatena M, Giachelli CM, Ross R, Raines EW. Apoptosis overrides survival signals through a caspase-mediated dominant-negative NF-kappa B loop. *Nat Cell Biol.* 1999; 1:227–233. [PubMed: 10559921]
22. Brand K, Eisele T, Kreusel U, Page M, Page S, Haas M, Gerling A, Kaltschmidt C, Neumann FJ, Mackman N, Baeurele PA, Walli AK, Neumeier D. Dysregulation of monocytic nuclear factor-kappa B by oxidized low-density lipoprotein. *Arteriosclerosis, thrombosis, and vascular biology.* 1997; 17:1901–1909.
23. Ross R. Atherosclerosis--an inflammatory disease. *N Engl J Med.* 1999; 340:115–126. [PubMed: 9887164]
24. Moulton KS. Plaque angiogenesis and atherosclerosis. *Curr Atheroscler Rep.* 2001; 3:225–233. [PubMed: 11286644]
25. Schutte HE. Plaque localization and distribution of vasa vasorum. A micro-angiological study of the human abdominal aorta. *Angiologica.* 1966; 3:21–39. [PubMed: 4160891]
26. Herrmann J, Lerman LO, Rodriguez-Porcel M, Holmes DR, Richardson DM, Ritman EL, Lerman A. Coronary vasa vasorum neovascularization precedes epicardial endothelial dysfunction in experimental hypercholesterolemia. *Cardiovasc Res.* 2001; 51:762–766. [PubMed: 11530109]
27. Lowensohn HS, Khouri EM, Gregg DE, Pyle RL, Patterson RE. Phasic right coronary artery blood flow in conscious dogs with normal and elevated right ventricular pressures. *Circ Res.* 1976; 39:760–766. [PubMed: 1000768]
28. Rakusan K, Flanagan MF, Geva T, Southern J, Van Praagh R. Morphometry of human coronary capillaries during normal growth and the effect of age in left ventricular pressure-overload hypertrophy. *Circulation.* 1992; 86:38–46. [PubMed: 1535573]

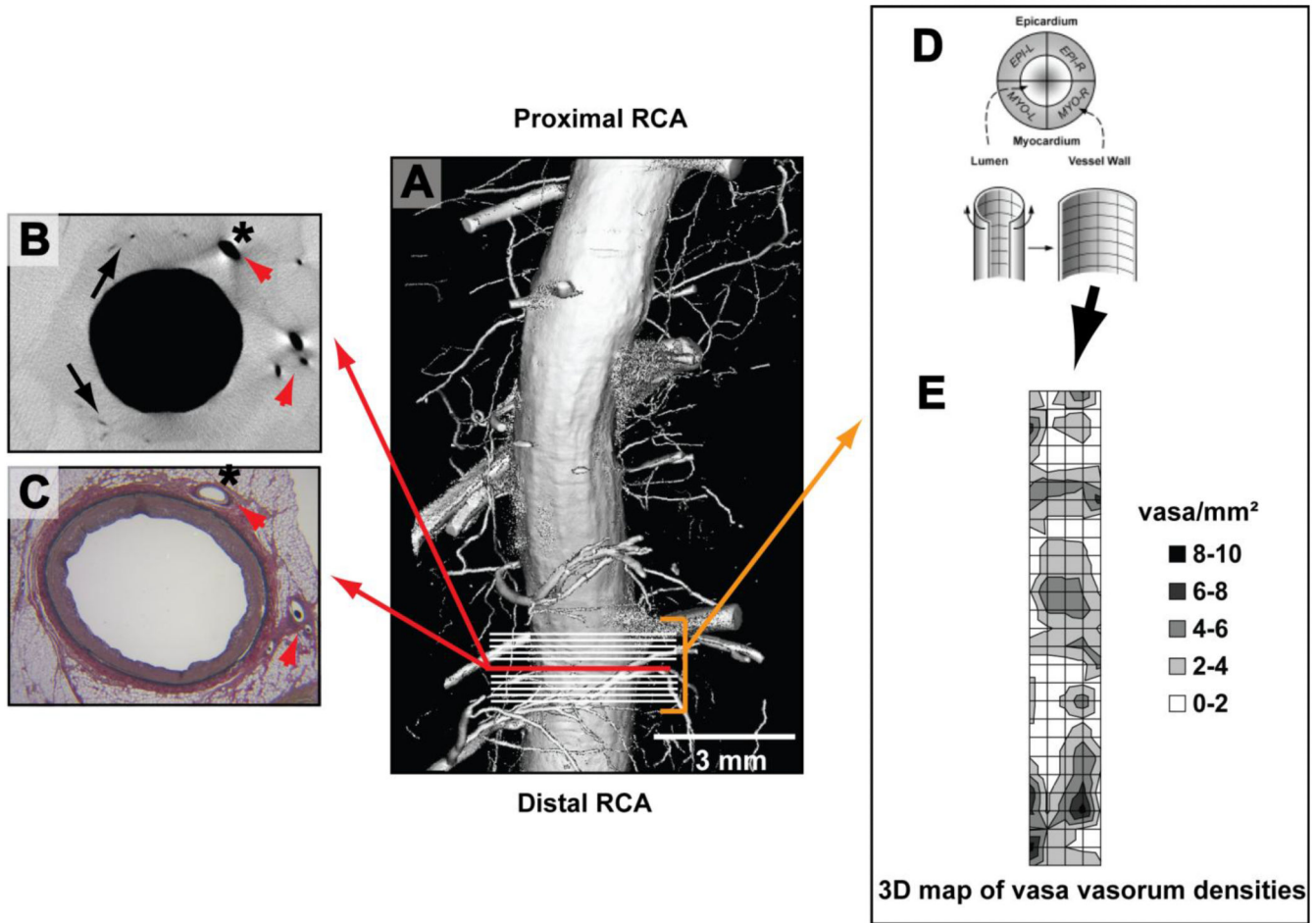


Figure 1. Methods

Panel A is a computer-generated surface display of a coronary artery lumen and its branches scanned with micro-CT. The upper-left panel B is a micro-CT cross-sectional image of that coronary and panel C is the corresponding Lawson’s Elastic van Gieson stained histology cross-section (the close match is appreciable by corresponding anatomical landmarks in both images [red arrow heads]). Vasa vasorum (black arrows) are differentiated from myocardial branches (*) by manually tracing the origin and destination of the vessels in hundreds of consecutive micro-CT images of the coronary. Next, vasa vasorum densities (vasa/mm²) are calculated in all four vessel wall quadrants (panel D; EPI-L stands for epicardial left quadrant) in ten, consecutive micro-CT cross sections (indicated by white lines in panel A) that are adjacent to the cross-section from panel B. Panel E: Calculated vasa vasorum densities (0 to 10 vasa vasorum per quadrant as indicated by the color-coded legend) are then displayed in a 3D map of vasa vasorum densities referenced to the endothelial surface⁴. The patchy spatial distribution of high and low vasa vasorum densities is reminiscent of the patchy distribution of atherosclerotic plaques. Finally, vasa vasorum densities and quantitative histology data (intima-media ratios and the number NF-κB and HIF-1α positive cells from three high-power fields per vessel wall quadrant) are correlated.

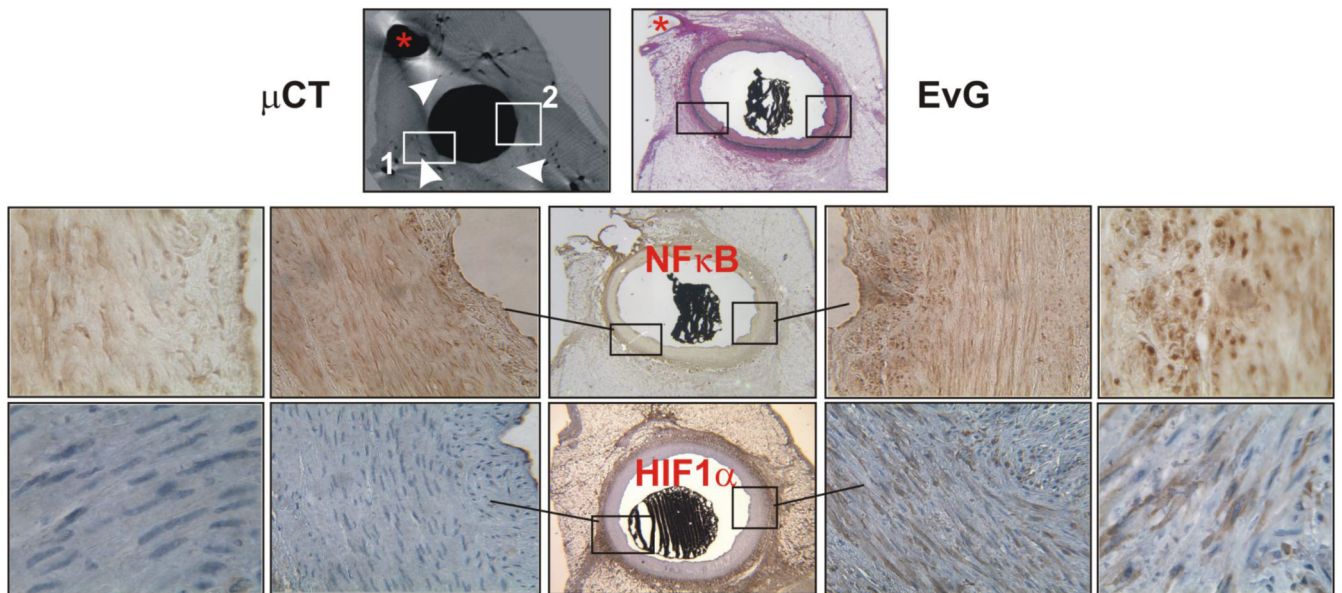


Figure 2.

Representative examples of corresponding micro-CT, Elastic van Gieson (EVG), NF- κ B, and HIF-1 α slides. Anatomical landmarks (*) helped to find corresponding slides. Two areas (white boxes, 1 and 2) from two different vessel wall quadrants are indicated in the micro-CT image and can be followed in the corresponding histological sections (sections stained for NF- κ B and HIF-1 α correspond to the upper micro CT and EVG sections; EVG, NF- κ B and HIF-1 α sections are adjacent to each other). (1) represents an area with a higher vasa vasorum density and shows less NF- κ B and HIF-1 α positive cells than (2) which represents an area with a lower vasa vasorum density. Vasa vasorum are shown as small black dots in the micro-CT cross-section because they are filled with contrast, the white arrowheads point at vasa vasorum; see also Figure 1. Magnifications, $\times 2$, $\times 40$, and $\times 125$.

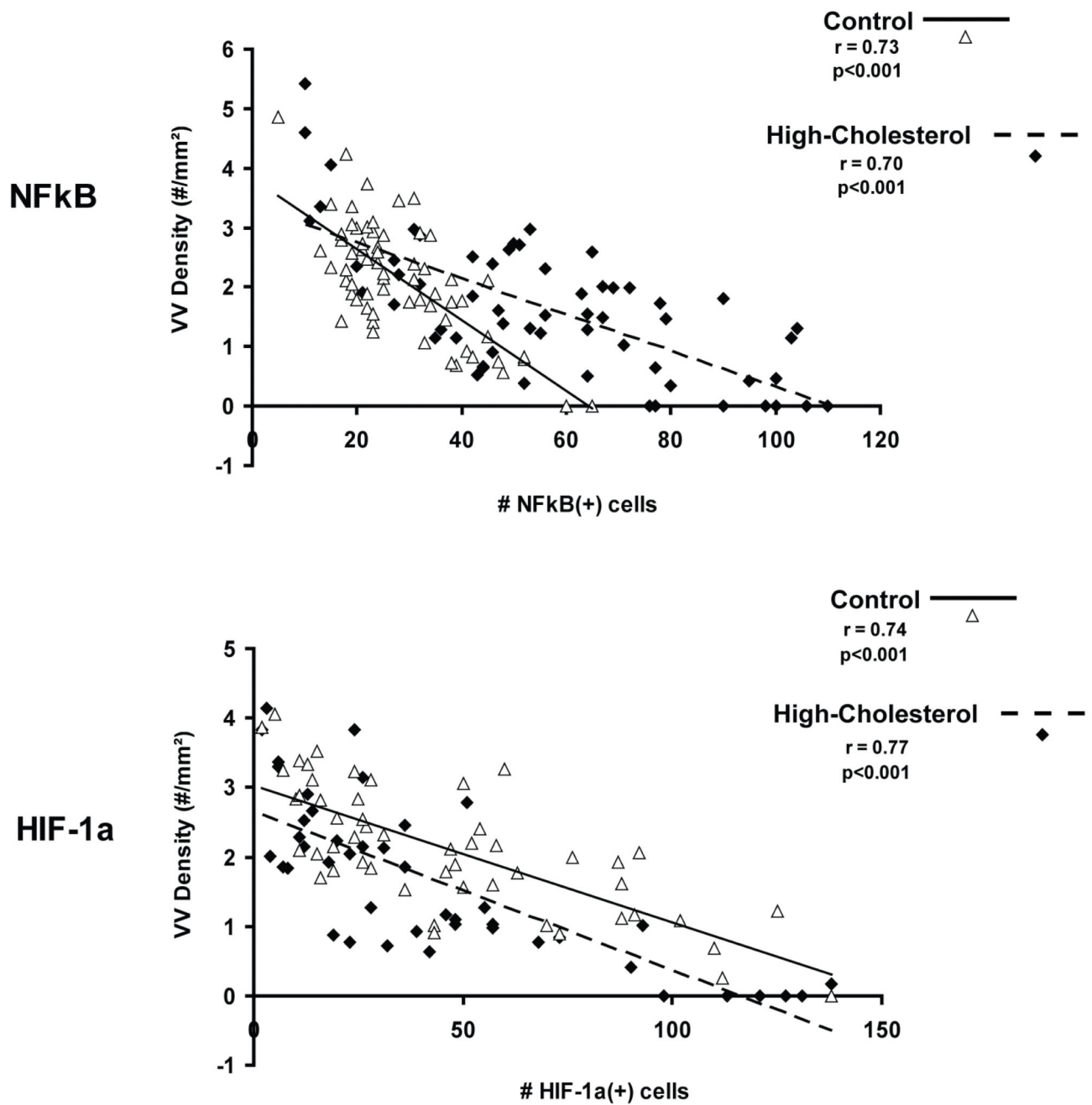


Figure 3.

Correlation between vasa vasorum spatial densities and NF- κ B and HIF-1 α in control and high-cholesterol RCAs. The graph shows that in both control and high-cholesterol animals there is a strong inverse correlation between NF- κ B and HIF-1 α positive cells and vasa vasorum spatial density.

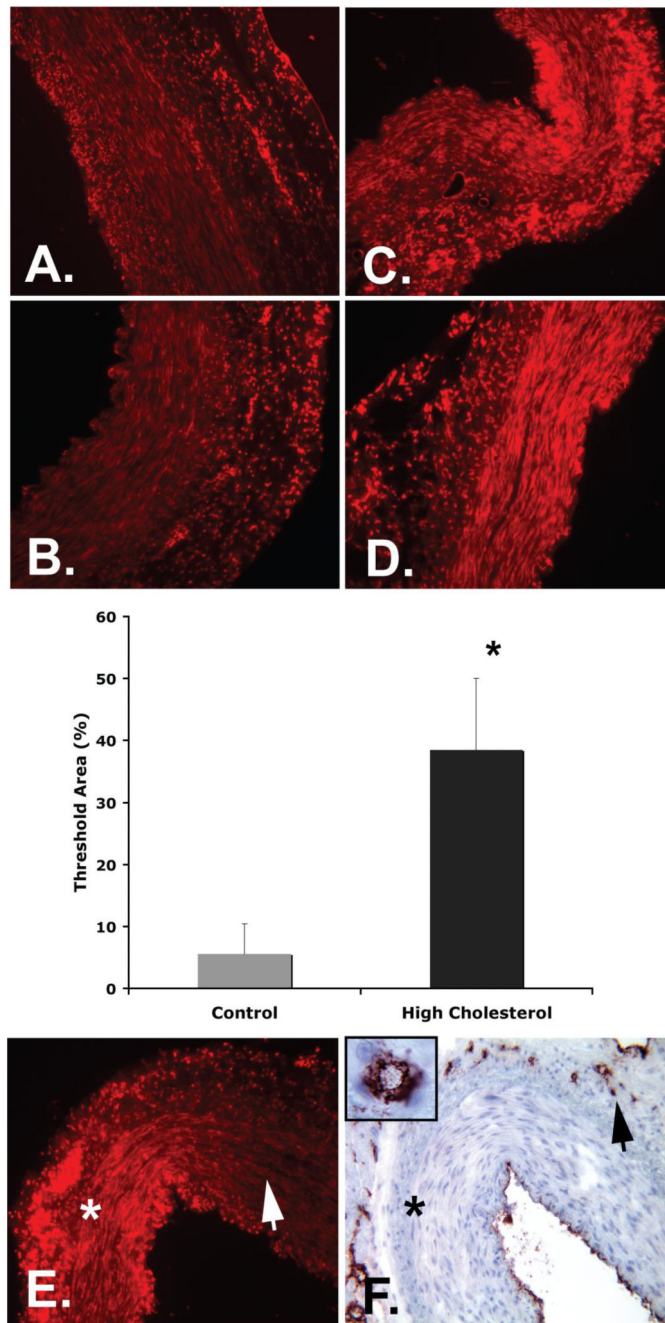


Figure 4. Dihydroethidium (DHE, orange/red) quantification in normal (A and B) and high cholesterol coronary arteries (C and D) shows significantly increased oxidative stress (increased expression of DHE) in hypercholesterolemic coronaries (mid panel, * $p < 0.001$). E, F: Representative examples showing that within one cross-section DHE expression was higher (panel E, marked by *) in vessel wall areas with low vasa vasorum densities (marked by * in panel F; vasa vasorum are indicated by the black arrow head and stained with factor VIII in

a corresponding section). In contrast, areas with higher vasa vasorum densities showed less DHE expression (white arrowhead in panel E). Magnification, $\times 20$ and $\times 100$.

TABLE

	Group N (n=6)	Group HC (n=6)
Heart Weight (g)	374±28	360±31
Total Cholesterol (mg/dl)	72±12	288±94 [*]
Low Density Lipoprotein (LDL)	36±9	171±68 [#]
High Density Lipoprotein (HDL)	33±4	118±36 [*]
Triglycerides	27±9	17±13
Blood pressure_{syst.} (mmHg)	127±16	121±18
Blood pressure_{diast.}	97±12	93±12
Heart rate (bpm)	79±17	72±14

Body and heart weights, lipid levels, and hemodynamic characteristics of normal (N) and hypercholesterolemic (HC) pigs.

^{*}P<0.001

[#]P<0.01.